IOP Publishing Biofabrication 13 (2021) 045028 https://doi.org/10.1088/1758-5090/ac26ac

Biofabrication

OPEN ACCESS

RECEIVED
24 February 2021

REVISED
8 September 2021

ACCEPTED FOR PUBLICATION
14 September 2021

PUBLISHED
27 September 2021

PAPER

Human iPSC-derived mesodermal progenitor cells preserve their vasculogenesis potential after extrusion and form hierarchically organized blood vessels

Leyla Dogan[1], Ruben Scheuring[2], Nicole Wagner[1], Yuichiro Ueda[1], Sven Schmidt[1], Philipp Wörsdörfer[1], Jürgen Groll[2,*] and Süleyman Ergün[1,*]

[1] Institute of Anatomy and Cell Biology, Julius-Maximilians-University of Würzburg, Koellikerstr. 6, 97070 Würzburg, Germany
[2] Chair for Functional Materials for Medicine and Dentistry at the Institute for Functional Materials and Biofabrication (IFB) and Bavarian Polymer Institute (BPI), University of Würzburg, Pleicherwall 2, 97070 Würzburg, Germany
* Authors to whom any correspondence should be addressed.

E-mail: juergen.groll@fmz.uni-wuerzburg.de **and** sueleyman.erguen@uni-wuerzburg.de

Keywords: vascular biofabrication, human iPSC-derived mesodermal cells (hiMPCs), extrusion of hiMPC-containing bioinks alginate + collagen type I, multilayered vessel wall with intimate, media and adventitia, vascular network and hierarchical organized vessels, electron microscopy, serial block face EM

Supplementary material for this article is available online

Abstract

Post-fabrication formation of a proper vasculature remains an unresolved challenge in bioprinting. Established strategies focus on the supply of the fabricated structure with nutrients and oxygen and either rely on the mere formation of a channel system using fugitive inks or additionally use mature endothelial cells and/or peri-endothelial cells such as smooth muscle cells for the formation of blood vessels *in vitro*. Functional vessels, however, exhibit a hierarchical organization and multilayered wall structure that is important for their function. Human induced pluripotent stem cell-derived mesodermal progenitor cells (hiMPCs) have been shown to possess the capacity to form blood vessels *in vitro*, but have so far not been assessed for their applicability in bioprinting processes. Here, we demonstrate that hiMPCs, after formulation into an alginate/collagen type I bioink and subsequent extrusion, retain their ability to give rise to the formation of complex vessels that display a hierarchical network in a process that mimics the embryonic steps of vessel formation during vasculogenesis. Histological evaluations at different time points of extrusion revealed the initial formation of spheres, followed by lumen formation and further structural maturation as evidenced by building a multilayered vessel wall and a vascular network. These findings are supported by immunostainings for endothelial and peri-endothelial cell markers as well as electron microscopic analyses at the ultrastructural level. Moreover, endothelial cells in capillary-like vessel structures deposited a basement membrane-like matrix at the basal side between the vessel wall and the alginate-collagen matrix. After transplantation of the printed constructs into the chicken chorioallantoic membrane (CAM) the printed vessels connected to the CAM blood vessels and get perfused *in vivo*. These results evidence the applicability and great potential of hiMPCs for the bioprinting of vascular structures mimicking the basic morphogenetic steps of *de novo* vessel formation during embryogenesis.

1. Introduction

Vascular disorders are the main reason for cardiovascular diseases (e.g. coronary artery disease) which are leading death cause worldwide. The favored clinical approach to overcome vascular failure is the transplantation of autologous vessel pieces as a vascular graft, e.g. using the internal thoracic artery or saphenous vein for coronary bypass surgery. Not only for the treatment of such vascular diseases but also for tissue regeneration and replacement the functional vascularization is an indispensable component for

achieving suited internal tissue structure in biofabricated cell-material composites. Hence, there is a huge need for approaches enabling the engineering of blood vessels regardless of which technology. The first steps of creating artificial blood vessels were undertaken by tissue engineering approaches, e.g. cell seeding into the decellularized matrix [1], annular mode casting [2] and seeding endothelial cells (ECs) into tubular structures that were created using collagen or collagen with some other matrix components like elastin [3–5]. Further attempts were made using biomaterials that were constructed as basic vascular structures and again seeded with multiple cell types [6, 7]. While these approaches resulted in tubular conduits, the spatial distribution of the used cell types as well as the scaffold architecture remained incomplete. More recently, bilayered small vessels were bioprinted using human umbilical vein endothelial cells (HUVECs) and smooth muscle cells (SMCs) [8].

Bioprinting is a novel promising option to create artificial blood vessels. While great progress has been made in the biofabrication of some functional tissues in the past decade [9–11], bioprinting of an appropriate vascular system beyond the mere generation of channel structures is still a big challenge. A scaffold-free tubular tissue was created using 3D-bioprinting of multicellular spheroids that were composed of HUVEC, aortic SMCs, and human dermal fibroblasts [12]. The functionality of these structures was tested *in vivo* after implantation into the rat abdominal aorta [12]. A few years later, the same group demonstrated the formation of tubular structures that were lined by ECs using bioprinting of a cellular mix composed of ECs, dermal fibroblast, and iPS-derived cardiomyocytes [13]. Recently, 3D bioprinting of a bilayered vessel-like tubular structure was demonstrated using the extrusion-based bioprinting of HUVECs and SMCs into gelatin methacryloyl (GelMA) as hydrogel with varying porosity [8]. This approach resulted in spatial separation of the printed cells in tubular structures that exhibited an inner layer containing HUVECs and an outer layer displaying SMCs. In another study, Zhou *et al* could print small vessels with two distinct cell layers by printing of ECs and SMCs within a bioink composition of GelMA, polyethylene-(glycol)diacrylate and alginate using an advanced coaxial 3D-bioplotter platform [14]. Several groups have utilized various techniques and mature cell sources to create vascular structures such as micro extrusion-based bio printing, cell sheet technology, electrospun scaffolding and coaxial cell printing [9, 10, 14–18].

While the aforementioned approaches delivered vascular-like 3D tubular structures, there are still major missing structural properties when compared to the vascular system *in situ*. The mature vascular system is composed of a complex network of various sized blood vessels that are organized in a hierarchical order: large or mid-sized arteries and veins are connected by microvessels such as arterioles, capillaries, and venules. Except for capillaries, all other types of blood vessels display a three-layered wall consisting of the innermost intimal layer that contains ECs, the media layer constructed of SMCs that provide the contractility of the vessel wall and finally the outermost adventitial layer [19, 20]. Capillaries also contain an intima that is lined by ECs and enwrapped by a discontinuous layer of pericytes from the outside. While both vascular intima and media are constructed by mature cells, the outermost vascular adventitia has been identified as a niche for vascular stem and progenitor cells (VW-SCs) that can deliver all vascular cells and even some types of blood cells upon activation, e.g. by angiogenic stimuli [19, 21–23]. Considering this complexity of the *in situ* vascular systems, it will probably not suffice when mature endothelial tubes alone or in combination with mature SMCs are printed.

In this current manuscript, we pursue an alternative approach for creating a complex and hierarchically organized 3D vascular network that resembles the vascular system as closely as possible *in situ*. Therefore, we used human iPSC-derived mesodermal progenitor cells (hiMPCs), that were shown to deliver both ECs and pericytes [24], instead of often used mature ECs, SMCs, or fibroblasts, and formulated them in alginate + collagen type I hydrogels. We then extruded these bioinks into molds to evaluate whether a *de novo* embryonic development of a vascular system can be achieved. We demonstrate here, that hiMPCs survive the extrusion into the alginate alone or alginate + collagen type I hydrogel and subsequently pass through a series of morphogenetic events under culture conditions starting mostly at culture days 5–6 after extrusion. These morphogenetic events begin with the formation of cell spheroids from which the nascent endothelial tubes form by self-assembly. These primitive vessel-like structures undergo several steps of further maturation and stabilization by assembling additional vascular mural cells such as pericytes or SMCs. Moreover, these vessel-like structures create a network that is composed of vessels showing different diameters and varying wall structures: capillary-like vessels displaying ECs, pericytes, and a basal lamina as well as three-layered vessel-like channels displaying an intima, media, and adventitia as evidenced by electron microscopic analyses. Consistent with these data, immunofluorescence analyses confirmed the luminal presence of $CD31^+$ ECs, that were covered by $NG2^+$ (pericyte marker) or a-SMA^+ (SMC marker) cells from the outside. Moreover, $CD34^+$ cells were found in the outermost layer of these vessel-like structures similar to the blood vessels *in situ* that harbor $CD34^+$ cells in their adventitial layer [25–27].

Taken together, this pioneering study reveals the suitability of hiMPCs for extrusion based bioprinting and elaborates suitable biomaterial properties that allow hiMPCs to unleash their vasculogenic potential closely mimicking basic steps of embryonic *de novo* vascular development. We show that hiMPCs have the capacity to deliver all vascular cell types which self-assemble into multi-layered vessel-like structures that are capable of forming a hierarchically organized vascular network.

2. Materials and methods

2.1. Cell culture

Human induced pluripotent stem cells (hiPSCs) and bioinks containing hiPSC-derived mesodermal cells (hiMPCs) [24] were used for the extrusion-based dispensing into silicone molds. The hiPSCs were generated from commercially available normal human dermal fibroblasts (juvenile NHDF, C-12300, Promocell, Heidelberg, Germany) by reprogramming, using either the hSTEMCCA-lentiviral construct [28, 29] or a Sendai virus reprogramming kit (CytoTune 2.0 Sendai reprogramming vectors, Ref#A16517; Lot#A16517, Invitrogen, Carlsbad, CA). hiPSCs were cultured on hESC-qualified Matrigel® (Corning, New York, NY, USA)-coated culture plates in StemMACS iPS Brew medium (Myltenyi Biotec, Bergisch Gladbach, Germany). The culturing media was changed daily. At 80%–85% confluency, cells were dissociated with StemPro® Accutase® (Thermo Fisher Scientific, Waltham, MA, USA) for 5 min at 37 °C and triturated to obtain a single cell suspension. hiPSCs were plated at a cell density of 2×10^4 cm^{-2} in StemMACS medium, supplemented with 10 μM ROCK inhibitor Y-27632 (Miltenyi Biotec) for the first 24 h after passaging. Basic characterization of the hiPSC line has been done by checking the expression of the pluripotency markers Oct4 and Sox2 (figures 1(A1)–(A3)) using immunofluorescence staining (IF)

Subsequently, the hiPSCs were converted to hiMPCs under directed differentiation conditions as recently published [24]. In brief, confluent hiPSCs were dissociated into a single cell suspension using Accutase and were counted. For mesodermal induction, 3.65×10^4 cm^{-2} hiPSCs were seeded on Matrigel-coated plates and cultured for one day in StemMACS iPS-Brew medium with 10 μM ROCK inhibitor (Y-27632). Subsequently, StemMACS iPS-Brew medium was replaced by mesodermal induction medium (Advanced DMEM/ F12, 0.2 mM L-Glutamine, 60 μg µl^{-1} Vitamin C, 10 μM CHIR 99021, 25 ng ml^{-1} BMP4) and the cells were cultured for further 3 d at 37 °C, 5% CO_2. The culture medium was changed daily. After 3 d of culturing in the mesodermal induction media, the cells were dissociated using Accutase and collected for extrusion-based dispensing of bioinks containing hiMPCs into the molds.

After extrusion, the cell-loaded discs were cultured with the specified medium at 37 °C, 5% CO_2. To induce the differentiation of the extruded hiMPCs into vascular cells e.g. ECs, a vascular differentiation medium containing hVEGF was used (Advanced DMEM/F12, FCS, Penstrep, 10 μM ROCK inhibitor (Y-27632), 0.2 mM L-Glutamine, 60 μg ml^{-1} Vitamin C, 50 ng ml^{-1} VEGF).

2.2. Hydrogel preparation and extrusion-based printing of hiMPCs

Sodium alginate (Sigma Aldrich, PH132S2) and collagen type I (Millipore, E2729) were used for bioink formulation. To prepare a 2% (w/v) alginate solution, sodium alginate powder was weighed, placed in a glass vial, and sterilized for 1 h under UV light. Then the sterilized powder was dissolved in PBS (Sigma-Aldrich) solution by stirring overnight at 37 °C. Collagen type I solution was dispersed in advanced DMEM, then 5N NaOH (Sigma, USA) was used to adjust the pH 7. All bioinks were stored in sterile conditions at the proper temperature. Before extrusion, hiMPCs were immediately dispersed within the advanced DMEM, and subsequently, this dispersion of cells was mixed with alginate carefully. Then this cell-loaded hydrogel mixture was loaded into syringes and subsequently extruded into the silicon molds to form spherical discs with 80 μl cell-loaded gel volume. In terms of using alginate + collagen type I hydrogel, the cell suspension was prepared at 4 °C using the appropriate amount of collagen type I. For each alginate + collagen type I-based experiment, the final hydrogel mixture was composed by 2% (w/v) alginate and 0.015% (w/v) collagen type I. The porosity of the alginate-based hydrogel was studied by Cryo-SEM (figure S1 (available online at stacks.iop.org/BF/13/045028/mmedia)).

The prepared collagen type I hydrogel + cell mixture was added to the alginate carefully. A homogeneous gel mixture was prepared by controlled up and down pipetting without creating bubbles and the bioink was immediately extruded under the same extrusion conditions as in pure alginate case. Different suspensions of hiMPCs (varying from 2.5×10^6 to 10×10^6 cells ml^{-1}) were mixed with the hydrogel. The cell-loaded gel was extruded through 25 G ¼ inch lock tip nozzle under a continuous pressure of 100 kPa. VIEWEG GmbH brand DC 200 model analog dispenser with timer was used to perform the experiments. The printed spherical discs were cross-linked using 20 mM $CaCl_2$ solution (Merck, EC:233-140-8) for 20 min. Then, the discs were washed with PBS and transferred into cell culture flask.

2.3. Chorioallantoic membrane (CAM) assay

Fertilized eggs were incubated for 3 days at 37.5 °C under 60% humidity in an egg incubator. Prior to

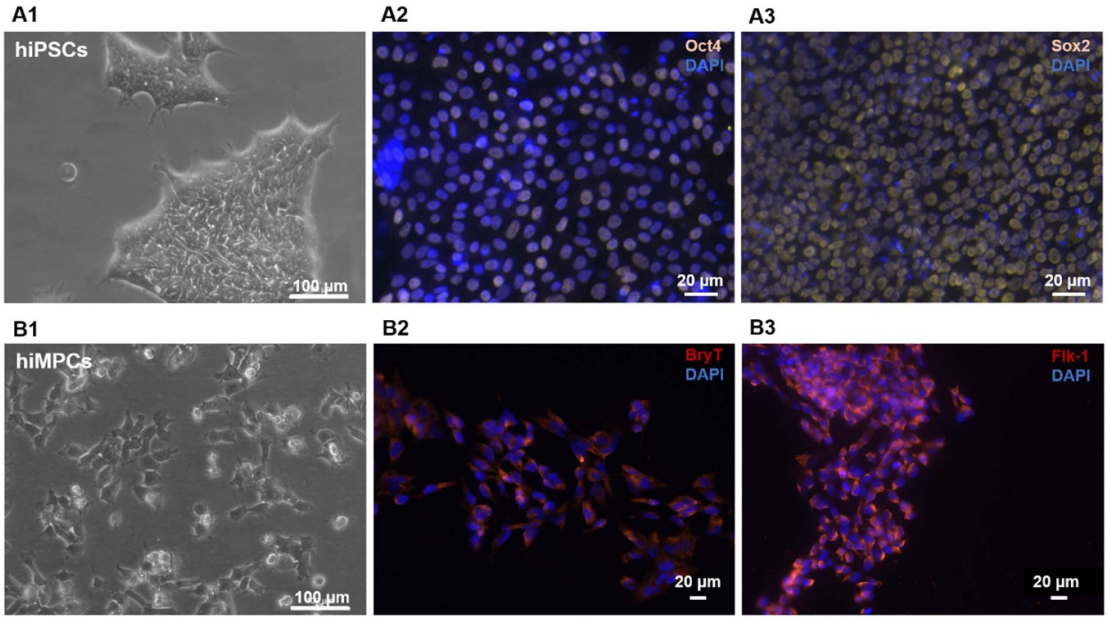

Figure 1. (A1) and (B1) Phase contrast microscopic images of hiPSCs and hiMPCs. Cells were cultured in standard 2D culture according to the protocol described in the materials and methods section. (A2) and (A3) Immunofluorescence staining of hiPSCs for Oct4 and Sox2. (B2) and (B3) Immunofluorescence staining of hiMPCs for BryT and FLK-1.

incubation, the eggs were carefully washed with sterile water. After three days, a small hole was punched in the bottom of the egg using a pair of sharp scissors and 5 ml albumen were removed using a syringe. Afterwards, a window (2 × 3 cm) was cut into the eggshell. The window was sealed with Tegaderm tape. The eggs were further incubated for 4–5 d at 37.5 °C under 60% humidity. Transplantation of printed scaffolds was conducted as follows: printed scaffolds (d14 samples) were transferred onto a sterile 6 mm diameter nylon mesh (150 μm grid-size, 50% open surface, 62 μm string diameter, 35 g m^{-2}, PAS2, Hartenstein, Germany) and covered with 50 μl matrigel solution. The samples were incubated for 10 min at 37 °C and 5% CO_2 for matrigel gelation.

During the gelation period, the desired site of transplantation on the CAM was carefully scratched using a pipette tip. Then the patches were placed onto the scratched part using sterile forceps, the printed sample facing the CAM. The eggshell was sealed using Tegaderm tape and incubated for additional 9 d at 37 °C under 60% humidity.

Finally, the transplanted samples were removed using surgical scissors and fixed immediately in 4% PFA solution. Subsequently, cryosections were performed for immunofluorescence analyses, immunohistochemistry as well as H&E staining.

2.4. Immunocytochemistry analysis

To characterize the cells before printing, the cells (cultured in 2D) were fixed with 4% paraformaldehyde (AppliChem, Darmstadt, Germany) in PBS for 15 min at room temperature (RT), then blocked with blocking buffer solution 5% NGS (Normal Goat Serum) for 1 h at the same temperature, in the presence of 0.1% Triton X-100 (Sigma–Aldrich) to permeabilize the cell membrane for detection of intracellular markers, or without Triton X-100 for detection of cell surface markers. Thereafter, the cells were incubated with primary antibodies in 2% BSA (Bovine Serum Albumin) + 1% NGS overnight at 4 °C. For immunocytochemical characterization of hiPSCs and hiMPCs following primary antibodies were used: Oct4 (Santa Cruz Biotechnology, sc-6279), Sox2 (R&D Systems, MAB2018), Brachyury (T) (R&D Systems, AF2085), Flk1 (Santa Cruz Biotechnology, sc-48161). Cells were incubated with primary antibodies overnight at 4 °C. The incubated samples were rinsed three times with PBS and exposed to appropriate fluorophore-conjugated secondary antibodies that were diluted in the PBS solution for 1 h at RT. Secondary Cy2-, Cy3- or Cy5-labelled antibodies were used to visualize primary antibodies. The immunostained samples were then studied microscopically and used for capturing pictures with a Biorevo fluorescence microscope (Keyence, Osaka, Japan). The analyses revealed that the hiMPCs express the mesodermal progenitor markers BryT and Flk1 (figures 1(B1)–(B3)).

For conventional histological analyses, the disc-shaped scaffolds were removed from the culture and washed in PBS 3× for 5 min. The scaffolds were fixed in 4% PFA that was freshly prepared in PBS for 24 h at 4 °C and then washed again 3× with PBS for 30 min to remove residual PFA. The fixed samples were stored submerged in 70% ethanol until embedding into the

paraffin. Afterward, paraffin sections were prepared with a required thickness (5–12 μm) and were then deparaffinized, rehydrated, and stained with hematoxylin and eosin (H&E) or Picrosirius red to visualize the collagenous matrix. For immunofluorescence analyses, antigens were unmasked using Sodium Citrate buffer (10 mM, pH 6). For immunostaining, the sections were exposed to antibodies for the following markers: CD34 (Miltenyi, 130-105-830), CD31 (DAKO, M0823), NG2 (Merck-Millipore, AB5320) (Abcam, AB5694). These markers are used the most for the detection and characterization of vascular wall cells. The stained sections were studied microscopically and used for capturing pictures by the Biorevo fluorescence microscope (Keyence, Osaka, Japan).

2.5. Transmission electron microscopy

Extruded discs were fixed in fixation solution (0.15 M cacodylate buffer pH 7.4 containing 2.5% glutaraldehyde, 2% formaldehyde with 2 mM calcium chloride) on ice for 2 h and washed 5 × 3 min in cold 0.15 M cacodylate buffer (50 mM cacodylate, 50 mM KCl, 2.5 mM $MgCl_2$, 2 mM $CaCl_2$ pH 7.4) on ice. Subsequently, specimens were incubated on ice in a reduced osmium solution containing 2% osmium tetroxide, 1.5% potassium ferrocyanide, 2 mM $CaCl_2$ in 0.15 mM sodium cacodylate buffer (pH 7.4). Specimens were washed with dH_2O at room temperature (RT) for 5 × 5 min followed by incubation in 1% thiocarbohydrazide solution for 25 min at RT. Specimens were washed with ddH_2O at RT, 5 × 5 min each, and incubated in 2% osmium tetroxide in ddH_20 for 30 min at RT. Afterward, specimens were incubated in aqueous UAR-EMS (4%, Uranyl Acetate Replacement stain, Electron Microscopy Sciences, Hatfield, USA) and stored at 4 °C overnight. The next day, specimens were washed 3 × 3 min in ddH_2O at RT. Prior to incubation with lead aspartate solution, specimens were washed 2 × 3 min in ddH_2O at 60 °C and subjected to *en bloc* Walton's lead aspartate staining [30] and placed in a 60 °C oven for 30 min. Specimens were washed 5 × 5 min with ddH_2O at RT and dehydrated using ice-cold solutions of freshly prepared 30%, 50%, 70%, 90%, 100%, 100% ethanol (anhydrous), 100% acetone (anhydrous) for 10 min each, then placed in anhydrous ice-cold acetone and left at RT for 10 min. Specimens were placed in 100% acetone at RT for 10 min. During this time, Epon812 was prepared. The resin was mixed thoroughly, and samples were placed into 25% Epon:acetone for 2 h, then into 50% Epon:acetone for 2 h, and 75% Epon:acetone for 2 h. Specimens were placed in 100% Epon overnight. The next day, Epon was replaced with fresh Epon for 2 h, and specimens were placed in Beam capsules and incubated in a 60 °C oven for 48 h for resin polymerization. For ultrathin sections, 70 nm thick ultrathin sections were cut with an ultramicrotome (Ultracut E, Reichert Jung, Germany) and collected on copper or nickel grids and finally analyzed with a LEO AB 912 transmission electron microscope (Carl Zeiss Microscopy GmbH, Germany).

2.6. Serial block-face electron microscopy (SBF-SEM)

For SBF-SEM, specimens were mounted on aluminium pins (Gatan Inc). The blocks were precision trimmed with a glass knife to expose the spheroids. Silver paint (Gatan Inc) was used to coat the edges of the tissue block to reduce charging during imaging using BSE mode using the variable pressure mode. Images were acquired using a scanning electron microscope (Sigma300VP; Carl Zeiss Microscopy GmbH, Germany) equipped with an automated ultramicrotome inside the vacuum chamber (3View; Gatan Inc). The ultramicrotome cut successive sections at a thickness of 50 nm. After each section, the sample block-face was scanned. The microscope, the stage, and the ultramicrotome were controlled using DigitalMicrograph software GMS3 (Gatan Inc). The SEM was operated in variable pressure mode (VP-Mode) The sample was scanned in VP-Mode with a chamber pressure of 15 Pa and landing energy of 3.5 kV. Imaging in VP-Mode reduced artifacts arising from sample charging due to high amounts of Epon between the spheroids.

2.6.1. Image processing and segmentation

Image alignment was performed using Digital Micrograph (Gatan Inc). Segmentation was performed using the TrakEM2 plug-in [31] of the open source image processing framework Fiji [32].

2.6.2. Data visualization

3D rendering model and movie (supplementary movie) were created using the open-source platform tomviz (https://tomviz.org/)

2.7. Cell viability

Live/dead cell staining was performed for testing the cell viability using Calcein AM (2 μM, C1430 Life technologies) and Ethidium Homodimer-1, EthD-1, (E1169, 4 μM, Life technologies) in accordance with the manufacturer's instruction. Briefly, three independently extruded discs were washed 3× by PBS for 5 min to remove the residual cell culture medium. Enough volume of freshly prepared staining solutions was added to cover the discs and then the discs were incubated at 37 °C for 30 min. Afterward, staining solutions were removed and replaced by PBS. The constructs were studied microscopically using a Leica PL microscope that is equipped with a digital camera allowing to capture pictures. In addition, to count the cells three independent scaffolds were dissolved by 2 ml of 20 mM EDTA for 10 min in RT and the cell suspension was further diluted with 5 ml PBS

before separating cells by centrifugation and dissociating them with 0.1 ml Accutase enzyme for 5 min (due to aggregation of cells). A sufficient amount of media was then added, and cells were carefully re-suspended and counted by Hemocytometer. The cellular behavior was followed by cell viability assays and the viability ratios were assessed at three incremental time points: 1, 3, and 7 d.

3. Results

The first aim was to generate mesodermal progenitor cells from hiPSCs [24]. After characterization of hiPSCs by detection of pluripotency markers Oct4 and Sox2 (figures 1(A1)–(A3)) using immunofluorescence staining (IF), the conversion of these cells into hiMPCs was performed under directed differentiation conditions according to a protocol previously established in our lab [24]. After 3 d of culturing in mesodermal induction media, the cells were dissociated using Accutase and IF detecting mesodermal progenitor cell markers such as vascular endothelial growth factor receptor 2 (FLK-1) and Brachyury were performed (figures 1(B1)–(B3)).

We then studied the behavior of hiMPCs after formulation into alginate-based bioinks and subsequent extrusion by a pressure-assisted dispersion technique through a nozzle system. Initial viability assessment demonstrated that cells survive this procedure at best within a sodium alginate + collagen type I bioink (figure 2(C)). After extrusion of the bioink containing hiMPCs into the silicone molds, the resulting constructs were cultivated in an ECs differentiation medium. To promote cellular survival and subsequent differentiation and to increase the number of vascular cells, particularly of ECs, further factors such as Vitamin C, Penicillin/Streptomycin solution, ROCK inhibitor, and particularly VEGF were added to the cell culture medium. The added factors are also beneficial for the induction, promotion, and maintenance of vascular morphogenesis including capillary-like tube formation [33, 34].

3D bioprinting techniques require bioinks that are biocompatible, non-immunogenic, and non-toxic, and further require cells that can deliver tissue- and/or organ-specific parenchymal cells which are able to enter tissue and organ morphogenesis. Alginate as a frequently used bioink attracts a lot of attention and is preferred by many groups not only for the features listed above but also due to its properties such as easy handling, fast cross-linking, controllable biodegradation as well as easy producibility [35]. The physical and chemical properties of the hydrogel should allow and support basic cellular behavior such as attachment to the matrix as well as cellular proliferation and differentiation. The structure and porosity of the alginate-based hydrogel was studied by Cryo-SEM (figure S1). Furthermore, the swelling and shrinkage properties of both alginate alone and alginate + collagen type I at different time points and with and without cells were analyzed and statistically evaluated (figure S2).

First, the extrusion process sodium alginate alone was chosen as bioink. Cells and biomaterials were mixed carefully, free from air bubbles, and placed into printing cartridge. The cell-loaded bioinks were extruded into disc-shaped silicon molds. During extrusion, cells are subjected to different shear stress within the nozzle. To reduce cell stress, it was necessary to determine the optimal nozzle size, suitable extrusion parameters, and most favorable cell density to preserve cell vitality and basic cellular behavior within the hydrogel after extrusion. To perform the extrusion, a homogenous, sterile hydrogel was prepared. Suspensions of hiMPCs were mixed with the sterile hydrogel and were extruded as described in material and methods under point 2.2. Cross-linked gel discs were transferred into cell culture flasks for further culturing as visualized in figure 2(B). The cells, extruded through 25 G ¼ inch lock tip nozzle, preserved their cellular viability and functionality.

Generally, extrusion of more than 5×10^6 cells ml^{-1} resulted in a cell survival time longer than 3 months within the alginate gel while morphogenetic events were limited. Extrusion of less than 2.5×10^6 cells ml^{-1} into alginate-based hydrogel alone resulted in a significant reduction of cellular survival time below 2 weeks. This indicates that a sufficient cellular density is needed in order to probably achieve a sufficient cell–cell communication within the hydrogel either by direct cell–cell interaction and/or in a paracrine manner via secreted factors from differentiating cells, e.g. ECs, pericytes or SMCs that might support the morphogenetic events and thus, also cell survival. In cases of using alginate + collagen type I hydrogel as bioink as mainly applied in the studies here, a cell density ranging between 2.5×10^6 and 10×10^6 cells ml^{-1} turned out to be optimal.

Then, we studied morphogenetic events under phase contrast microscopy. We observed the formation of 3D cell spheres in both alginate-based bioink alone and alginate + collagen type I hydrogel starting around culture day 5–7. However, a network of elongated and enlarged cell cords was only observed in alginate + collagen type I hydrogel (figures 2(D) and 3(A)). It is well described that *de novo* development of blood vessels during the embryogenesis starts also with the formation of spherical cell aggregates by specialized mesodermal progenitors that form the so-called 'blood islands', that serve as the source for both endothelial and hematopoietic cells [36, 37].

As a biomaterial, alginate turned out to be suitable for keeping hiMPCs viable. However, the gel is mechanically tough and not adhesive enough to provide cell attachment. For that reason, it did not support

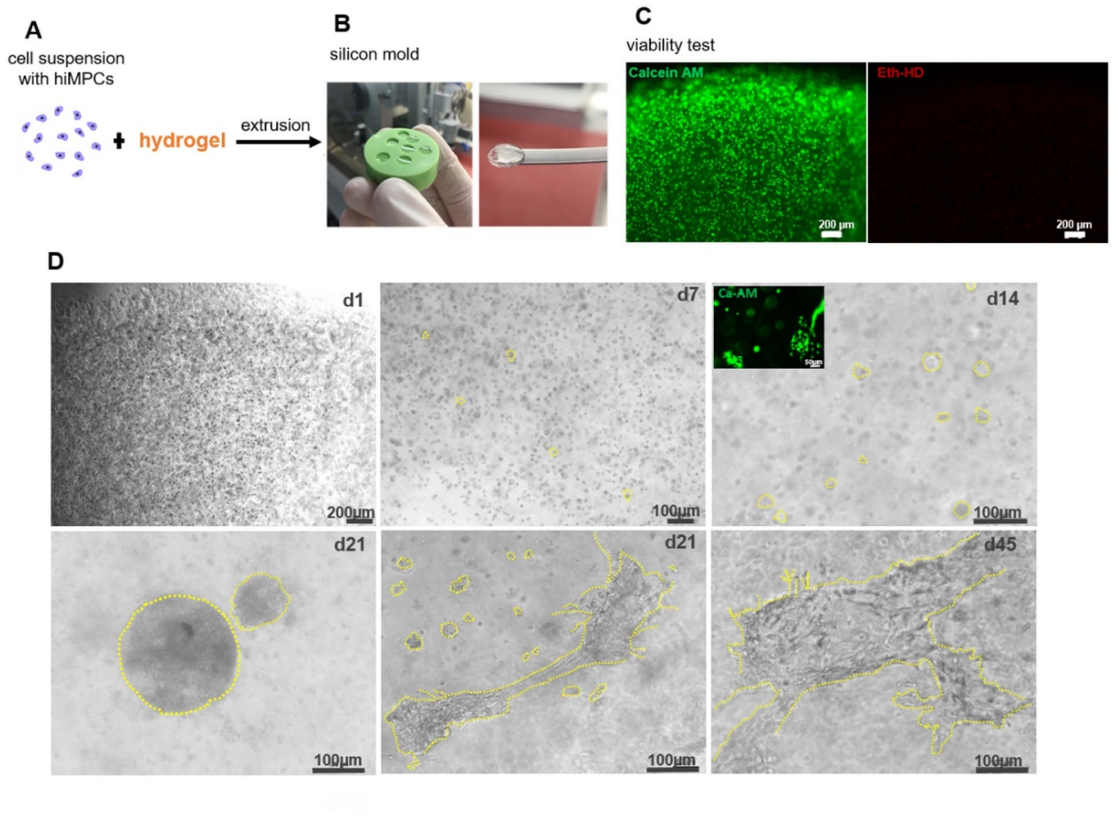

Figure 2. Extrusion-based dispensing of bioinks containing hiMPCs into silicone molds, initial viability test and phase contract microscopic study of cultured constructs (A). Cell suspension of hiMPCs formulated into alginate alone or alginate + collagen type I as bioink, (B). Disc form after extrusion into the silicon molds (C). Initial viability testing by application of Calcein-AM and EthD-1. (D) Phase contrast microscopy of cultured constructs at different culture time points as indicated. Morphogenetic events with single cells at day 1, small cell spheres at day 7, large spheres and cell cords at day 14, different sized spheres and cell cords with branching at day 21 and large branching cell cords at day 45.

cell migration, a process that is essential for initiating vascular morphogenesis. To this end, we decided to modify the alginate bioink by blending with collagen type I to support the cellular migration, proliferation and thus, morphogenetic events. Indeed, phase contrast microscopic observation at culture days 7–9 after extrusion revealed elongated cell cord formation and morphogenetic processes including the formation of a vessel-like branching pattern. These data suggest that the hiMPCs actually require the presence of collagen type I to migrate, proliferate, interact and form 3D structures within the alginate-based hydrogel. hiMPCs containing collagen type I gelation should be dispensed into alginate as fast as possible in order to avoid non-homogenous dispersion of the bioink. This critical parameter should be considered while preparing cell-loaded gel prior to extrusion.

These results clearly suggest that the The viability analyses using Calcein AM at three incremental time points: 1, 3, and 7 d, allowed beside the cell survival assessment also to follow some morphogenetic events such as the formation of cell spheres, cell cords and their branching pattern and the formation of hollow and tubular structures (figures 3(A)–(C)).

These results clearly suggest that the enrichment of alginate with collagen type I results in a cell responsive bioink that supports cell attachment, cell migration and cell–cell as well as cell–gel interaction better than alginate-based hydrogel alone. Moreover, the elongated cords displayed network formation to some extent (figure 3(C)). To this end, almost all basic steps that are needed for vascular morphogenesis and vessel network formation were achieved using alginate plus collagen type I as bioink. Furthermore, the optimal extruded cell density reduced the adverse effect on cell viability and survival and resulted in an improvement of the aforementioned parameters in a ratio up to >75% (figures 3(B) and (C)).

In order to better study the mentioned morphogenetic events, the printed constructs were embedded in paraffin and cross sections (10 μm) of these tissue blocks were used for H&E staining. Light microscopic analyses revealed time-dependent morphogenetic changes. The cultures started with single cells distributed randomly within the gel at culture day 1, followed by the formation of cell spheroids at day 10 and a branching vascular-like channel system at day 25 after bioprinting (figure 4(A)). These morphogenetic steps clearly suggest that hiMPCs recapitulate a

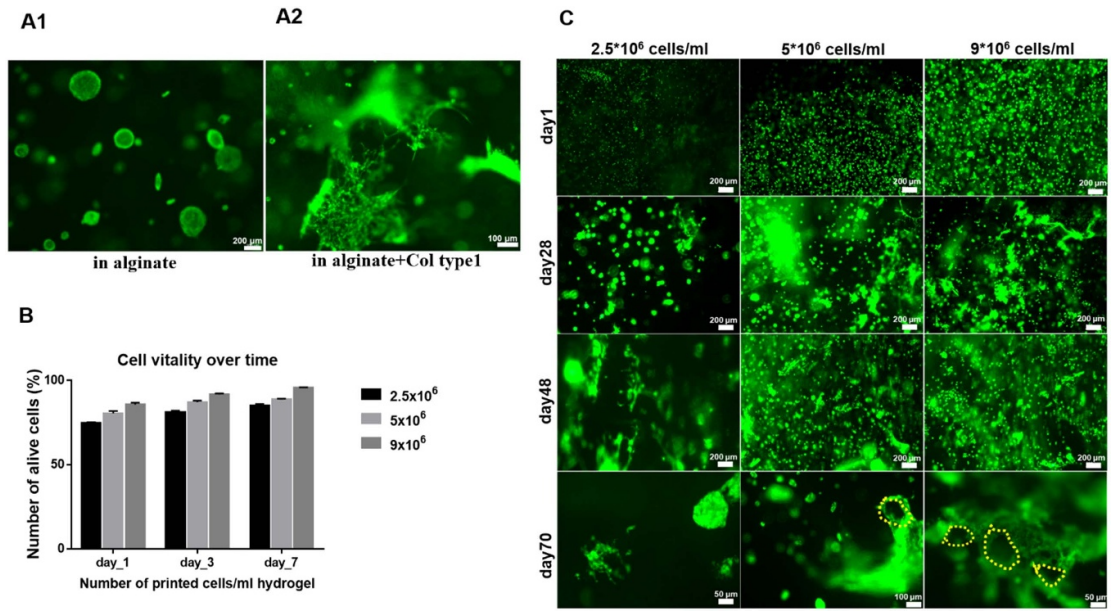

Figure 3. (A) Calcein-AM-fluorescent cell viability images of the extruded cells (A1) in alginate at day 100 and (A2) in alginate + collagen type I at day 70. (B) Percentage of live cell counts of the extruded cells within alginate + collagen type I hydrogel at culture day 1, 3 and 7 (bar colors indicate the cell density). Cell vitality data were generated from three independent printed discs. Error bars from statistical analysis indicate SDs. *P* values were calculated by unpaired Student's *t*-test. $^{*}p \leqslant 0.05$, $^{**}p \leqslant 0.01$ $^{***}p \leqslant 0.001$, n.s.: non-significant. (C) Fluorescent cell viability images of the extruded hiMPCs at different density within alginate + collagen type I hydrogel. The extrusion parameters: 25G (ID = 340 μm) ¼" nozzle, one bar, RT, into silicone mold. Yellow dotted lines mark hollow structures formed by hiMPCs that are already visible after Calcein-AM fluorescent labelling.

differentiation program that is well known from the *de novo* embryonic vascular development by vasculogenesis as described previously [38]. Remarkably, lumen formation within cell spheroids can be detected already at culture days 7–10 (figure 4(A)). These events are progressing with further culture time and result in (a) stabilization of the wall of the vessel-like channels, e.g. by assembly of peri-ECs into the wall and (b) branching, probably due to angiogenic sprouting of new vessels from the already formed ones as visualized by H&E staining at day 14 (figure 4(A)). The flattened and elongated nuclei of cells lining the luminal surface indicate their EC-like identity. The H&E stained inset in figure 4(A) that was captured from a section of day 21 after extrusion clearly displays lumen formation and a multilayered vessel-like wall structure (figure 4(A)). Furthermore, the paraffin sections were also stained with Picrosirius red in order to visualize the collagen matrix (figure 4(B)). This staining revealed a dense deposition of collagen around the vascular-like branching network that also enabled the recognition of lumen formation in some areas of this network. We assume that this densely deposited collagen reflects not only the collagen type I that was added to hydrogel but also collagen components that were produced by the cells themselves while forming vessel-like structures.

During blood vessel formation, endothelial progenitor cells called angioblasts emerge as scattered cells in the mesoderm and aggregate to form cords that predetermine future blood vessels. The ECs that are derived from these progenitors reorganize into blood-carrying tubes forming a primary vascular plexus by a process that is termed vasculogenesis. Subsequently, this initial primary vascular network is remodeled and extended by mechanisms that govern the further vascular maturation up to formation of a hierarchically organized vascular system [38–40]. VEGF signaling through the VEGF receptors-1 and -2 is the major mechanism that regulates almost all aforementioned steps of vascular formation and remodeling in health and diseases [41]. Thus, we added VEGF in all stages of culturing the extruded constructs containing hiMPCs. In addition to increase the cell–cell interactions which is required throughout the formation of the vasculature and must occur in a precise spatiotemporal sequence [42], the constructs were cultured in endothelial growth medium. Moreover, signaling of non-ECs, e.g. peri-ECs in a close vicinity to the ECs as well as signals from the extracellular matrix are crucial for maintenance and further maturation of newly created blood vessels [43, 44]. Our data clearly suggest that such processes, mechanisms of cell-cell- and cell-matrix-interaction are not only essential in *in vivo* vascular formation but also indispensable for vascular bioprinting.

The basic indispensable step of vascular maturation is the tight integration of peri-ECs such as pericytes and SMCs into the vessel wall [33].

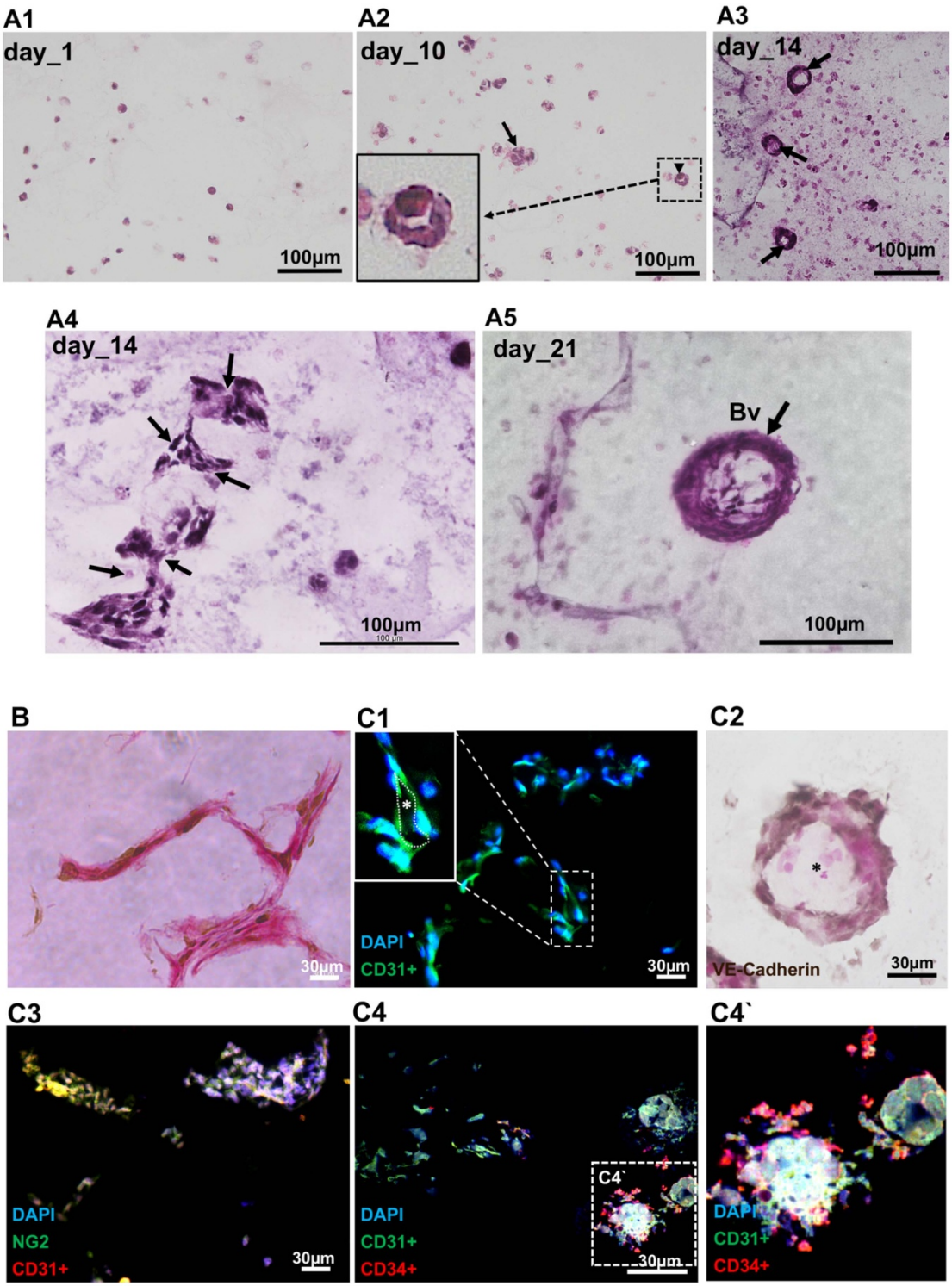

Figure 4. (A) H&E staining of extruded constructs of alginate + collagen type I hydrogel containing hiMPCs at days 1, 10, 14, and 21 of culture. Single cells at day 1 (A1), formation of spheroids (arrow, A2) and small vessel with lumen (arrowhead, A2 and inset in higher magnification) at day 10, the formation of vessel-like structures (arrows, A3), connected and branching small vessels (arrows, A4), relatively large vessel with multilayered wall structure (Bv, A5). (B) Picrosirius staining of the extruded constructs after 2 weeks demonstrating vessel-like network formation. The image was taken with 40× magnification. (C) Immunostaining on sections of the extruded constructs of hiMPCs with alginate + collagen type I hydrogel. Immunostaining for CD31 alone (C1, green and DAPI in blue for cell nuclei staining) with inset in higher magnification showing lumen formation (*) by CD31-postive cells, and VE-cadherin alone (C2, DAB staining in black, and counterstaining Calcium red for cell nuclei staining), (*) marks lumen with VE-cadherin-negative cells that are not integrated into vessel formation, CD31 (red) and NG2 (green) double staining (C3), CD31 (green) and CD34 (red) double staining (C4) and inset from the marked area of C4 in higher magnification (C4') showing lumen formation by CD31-positive cells while CD34-positive cells are localized around the constructs.

Next, we wanted to improve this step, in order to achieve a multilayered vessel wall and thus varied the number of cells being extruded in bioprinting. These analyses revealed that increasing the density of hiMPCs, e.g. up to 9×10^6 cells ml^{-1} resulted in formation of vessel-like channels of different size. A part of these channels displayed a multilayered wall structure. Of note, extrusion of hiMPCs at a density of 2.5×10^6 cells ml^{-1} resulted in capillary-like microvessels missing a multilayered wall structure and the vessel formation took place after a significantly longer period (almost 2 months). These data underline again the impact of using an optimized cell density in the bioprinting of blood vessels.

Next, we wanted to characterize the cells forming the vascular-like channels at the immunophenotypic level using immunostaining on paraffin sections for markers that are specific for ECs such CD31, for peri-ECs such as NG2 and αSMA, and for vascular progenitor cells such as CD34 [21, 22, 45, 46], The presented results demonstrate that indeed all vascular cell types are present in the wall of the vascular-like channels developed after extrusion of hiMPCs into the alginate + collagen type I hydrogel (figure 4(C)). Moreover, the spatial organization of these cell types within the wall of vessel-like channels was very similar to that *in vivo* as $CD31^+$ ECs lined the luminal surface of the vascular channels, the $NG2^+$ or αSMA^+ cells were found to cover the endothelial layer from outside and more surprisingly a part of $CD34^+$ cells was found in the outermost layer of the vessel wall, again similar to the adventitial layer of blood vessels *in situ* (figure 4(C3)).

Based on the aforementioned results from histological and immunohistological studies, we aimed at analyzing these vascular channels in more detail at the ultrastructural level using electron microscopic imaging via TEM and serial block-face REM. These analyses confirmed entirely our histological observation suggesting the presence of a whole spectrum of vessel types representing different parts of the vascular hierarchy such as capillaries with and without pericyte coverage and basement membrane as well as large and mid-sized vessel-like channels that displayed a multilayered vessel wall (figure 5). Already in toluidine blue-stained semi-thin sections of our constructs revealed capillary-like structures exhibiting cells lining the lumen (intima) and a cell that covered this endothelial lining from the outside (figure 5(A)). Moreover, the morphological appearance of these covering cells is similar to the pericytes *in situ* (figures 5(A) and (C1)). As also visualized in the same figure panel, some capillaries are constructed by ECs only (figures 5(A), (B2) and (B3)). Since we observed such structures in almost all tissue blocks, we assume that the vessel formation is taking place in a relatively large area within the alginate + collagen type I hydrogel. The subsequently performed electron microscopic analyses confirmed these observations at the ultrastructural level (figures 5(B) and (C)). Some capillary-like channels displayed less flattened cells indicating that they are structurally still at an immature state (figure 5(B)). More mature capillary-like vessels displaying endothelial and peri-ECs were also observed (figure 5(C1)). Higher magnification revealed that the EC layer is anchored at a basal lamina-like condensed matrix that is tightly attached to the basal side of the intimal layer (figure 5(C2)). Moreover, confirming our histological analyses on paraffin sections, also TEM studies revealed that a part of blood vessels displays a multilayered wall structure (figures 5(C3)–(C5)). We could identify at least three concentric layers: the innermost intima that is followed by media and the outermost adventitia as presented in different magnifications (figures 5(C3)–(C5)). Furthermore, the section morphology of the cells in these layers clearly visualize that ECs are more oriented in the long axis of the channel, the media cells are oriented circularly and the adventitia-like cells display many thin processes that are embedded in a collagen matrix that is apparently structured by the vascular wall cells (figures 5(C3)–(C5)).

In order to better visualize the vessel-like lumen formation we used serial block-face electron microscopy (SBF-SEM) and performed 3D reconstruction about a distance of 7.5 μm (figure 6). These analyses revealed that hiMPC-derived vascular cells formed complex lumen with branching pattern that is provided by thin cellular processes, which subdivide a lumen into two further lumens and by this, create a complex communicating channel system. While the further maturation of these channels depends on perfusion and further vascular maturation, these data demonstrate morphogenesis of vessel-like lumen and their branching, e.g. similar to the vessel branching processes *in situ* [47, 48].

Next, we transplanted the printed vessel constructs into the chicken embryo chorioallantoic membrane (CAM) in order to test their perfusion capacity as we successfully performed using vascularized organoids [24, 49]. At days 7–9 the transplanted patches containing printed constructs were removed and used for preparation of tissue sections that were processed for immunostaining using human specific CD31 antibody and αSMA antibody (figures 7(A)–(L)). The printed vessels were perfused by chicken blood (figure 7(C)). Immunostainings revealed human specific CD31-postive vessels of different diameter (figures 7(D)–(F)). In double immunostainings for CD31 and αSMA we could detect CD31-positive endothelial lining of the printed vessels in different diameter that were (a) surrounded by SMCs and (b) perfused by chicken nucleated (DAPI marked) red blood cells

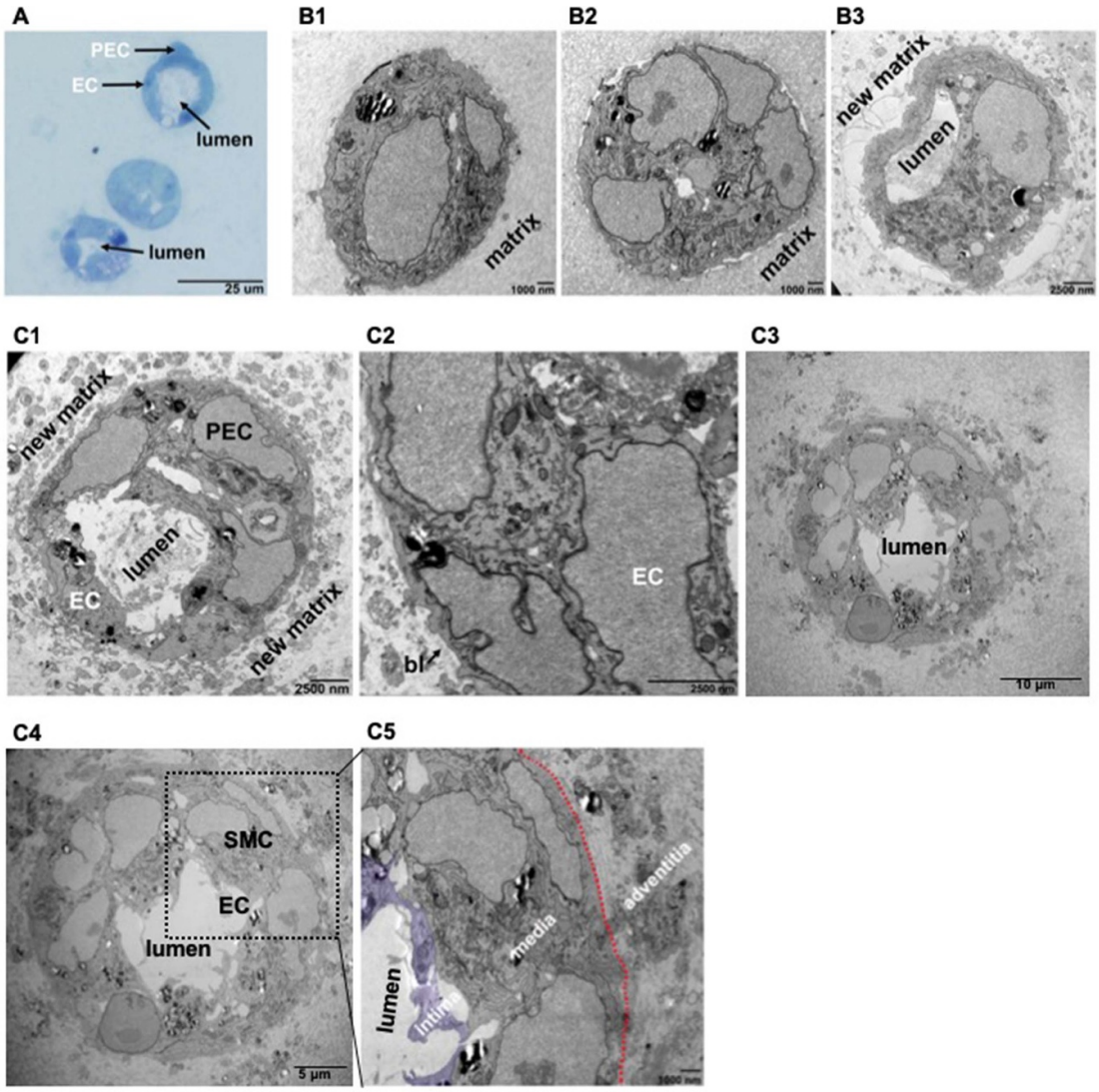

Figure 5. Semi-thin sectional and ultrastructural evaluation of vessels generated by extrusion-based shape-free printing of hiMPCs with alginate + collagen type I hydrogel into a silicone mold. (A). Semi-thin section analyses results after toluidin blue staining (1 μm sections) display vessel-like tubes lined by ECs and PEC (peri-endothelial cell, e.g. pericyte). (B). Electron microscopic analyses show single cells (B1), cell spheroid (B2), and a capillary that consist of only a single layer of ECs forming a lumen and new extracellular matrix surrounding this capillary (B3). (C). Electron microscopic studies show vessels with ECs and PECs. Capillary-like vessel with ECs and PEC and new matrix deposition around these vessels (C1). Blood vessel with the single innermost layer of ECs that is covered by single PEC form outside and that in turn is underlined by a basal lamina as indicated (arrow and **bl**) (C2), entire cross section of a multilayered blood vessel in lower (C3) and higher magnification (C4) with innermost endothelial cells (EC) and concentrically organized smooth muscle-like cells (SMC). Higher magnification of the marked area (rectangle) in C4 showing the innermost intima (marked by purple color), two-three concentric cell layers of media and the outermost adventitia as separated from the media by the dotted red line (C5).

(figures 7(G)–(L)) suggesting the connection of the printed vessels to the chicken blood vessels *in vivo*.

4. Discussion

The presented data demonstrate the artificial generation of a hierarchically organized vascular system after extrusion by combining vascular stem cell technology with bioprinting technology that allowed us to mimic the basic steps of *de novo* vessel formation during embryogenesis. Briefly, we demonstrate, as also summarized in the graphical representation (figure 8), that (a) hiPSC-derived mesodermal cells (hiMPCs), that were recently shown to have a vasculogenic potential [24] were formulated into hydrogels composed of alginate alone or alginate + collagen type I hydrogel and sub-sequently survived the extrusion-based dispensing into a silicon mold, (b) 7 d after extrusion hiMPCs differentiated and underwent morphogenetic events such as formation of 3D spheroids in several places within the hydrogel, (c) few days after spheroid formation, elongated cell cords emerged that displayed also morphological features of branching and network formation, e.g. connecting neighboring spheroids, (d) at culture days 15–21 the 3D cell cords were enlarged

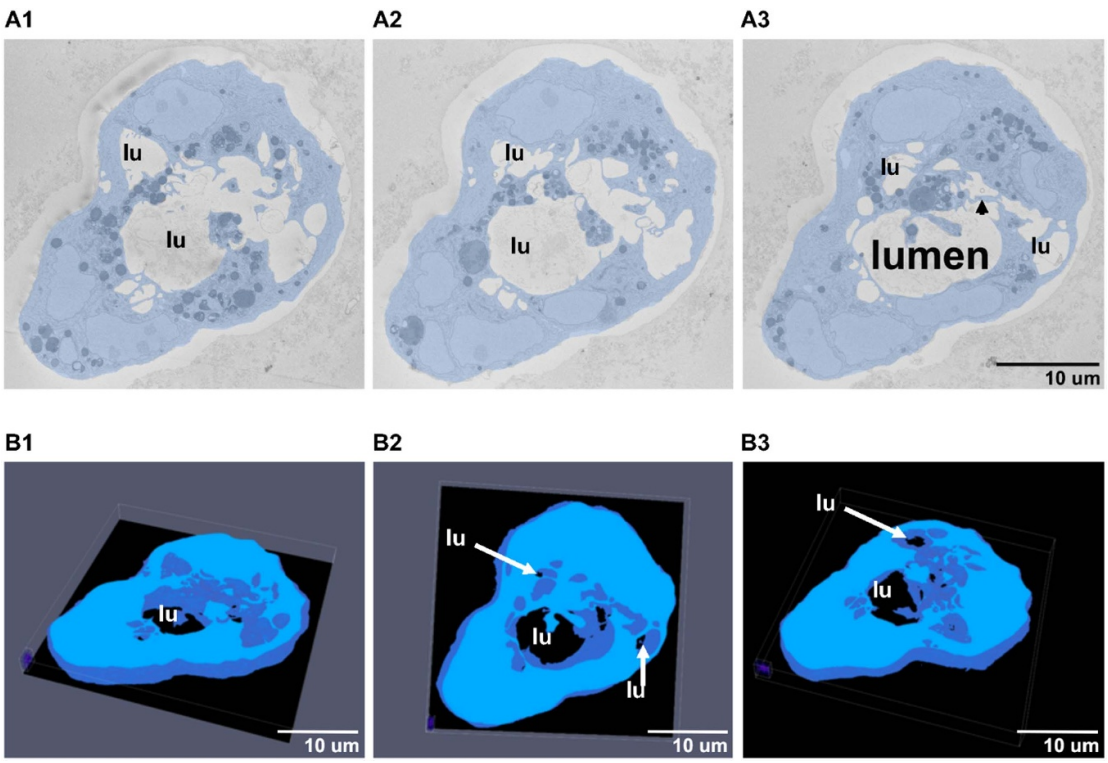

Figure 6. SBF-SEM imaging of branching lumen (**lu**) formation by hiMPC-derived vascular cells after extrusion into silicone molds. (A1)–(A3) Selected images from single SBF-SEM slices showing hiMPC-derived endothelial-like cells (blue) that form a complex lumen (lu) with thin cellular processes leading to lumen branching (arrowhead, A3). (B1)–(B3) Large-volume reconstruction of the SBF-SEM slices presented in (A) showing the branching pattern by thin processes of endothelial-like cells that separate the lumen (**lu**) from each other. SBF-SEM dataset: Reconstruction of a 7.5 μm volume: 151 sections, 10 × 10 × 50 nm voxel size. Source data are available for this figure. Scale bars as indicated.

displaying more complex branching and networking, (e) conventional histological H&E staining on paraffin sections of the aforementioned constructs revealed vessel-like channels, (f) immunostaining of the sections for the endothelial marker CD31 and CD34 as well as for NG2 and aSMA as pericyte and smooth muscle cell marker confirmed the vascular nature of the channels and the right spatial organization of endothelial and peri-endothelial cells in their wall, (g) electron microscopic studies of these constructs revealed capillaries, small vessels with single peri-endothelial cells and larger vessels with three-layered wall structure such as intima-, media- and adventitia-like layers, (h) SBF-SEM analyses with segmentation and 3D reconstruction revealed vessel-like lumen formation that is subdivided into two further lumens by cellular processes which create a communicating vessel-like channel system and finally (i) the printed vessel displayed blood perfusion capacity *in vivo* after transplantation into the CAM.

The present data suggest that using vascular progenitors that can deliver all mature vascular wall cell types such as ECs, pericytes, SMCs and mesenchymal cells or fibroblasts in biofabrication of blood vessels is a promising approach to generate an artificial vascular system in bioprinted tissues and organs. At the biological level, this approach uses (a) the vasculogenic potential of the vascular progenitor cells instead of using mature vascular cells, and (b) mimics the embryogenesis of blood vessels by combining the aforementioned cellular potential with material and the techniques of biofabrication to achieve not only a rigid pipe but also rather plastic and adaptable vessel system.

Tissue vascularization is an indispensable prerequisite for the proper development and function of tissue as well as organ. The primary hypothesis of the present work was to test the capacity of vascular progenitor cells to form vessel-like structures by self-assembly after being formulated in bioink, e.g. alginate + collagen type I hydrogel and subsequent extrusion into a silicon mold as performed here. We chose this setup to unambiguously explore whether the hiMPCs do the expected job after being exposed to shear stress through a syringe and within a matrix that is different from the matrix *in situ*. Furthermore, our second aim was to test to which extend the hiMPCs can enter into morphogenetic events within the hydrogel, there needed for the formation of vessel-like structures. Moreover, the best-desired outcome would be the formation of blood vessels that exhibit (a) different sizes, e.g. capillaries and larger vessels, (b) a multilayered wall structure, and (c) a vascular network that is organized in hierarchic manner

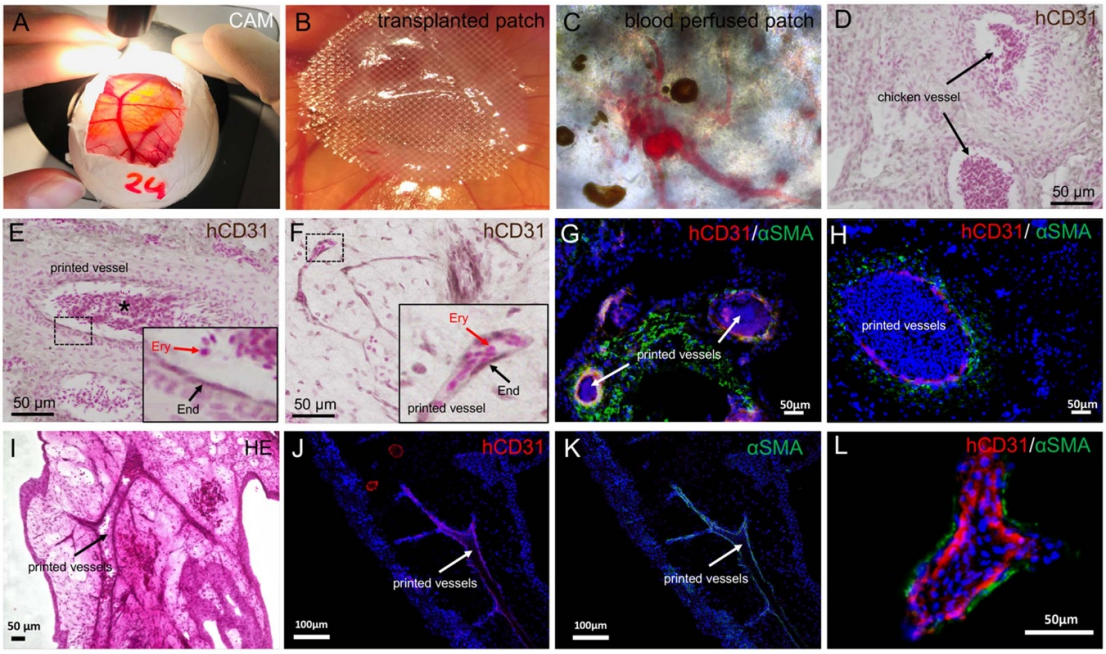

Figure 7. Transplantation of printed vessels into CAM and *in vivo* blood perfusion. CAM vessels that are visible in an opened window on chicken egg shell (A). Transplanted patch (mesh structure) containing printed constructs with vessels (B). Under *in vivo* conditions blood perfused vessels in transplanted patch suggesting the connection of the printed vessels to the CAM vessels (C). No detectable CD31 immunostaining (with Calcium red counterstaining) in the chicken blood vessels of CAM used as negative control for human specific CD31 antibody (D). Human specific CD31 immunostaining in endothelial cells lining the lumen of a transplanted vessels as clearly visualized in inset (black arrow and 'End') with higher magnification (E). Note the thickness of the vessel wall in inset and perfusion of the printed vessel by nucleated chicken red blood cells (red arrow and 'Ery') (E). Immunostaining for human specific CD31 in small and mid-sized vessels in network formation (F), inset of F: CD31-positive endothelial cells (black arrow and 'End') and nucleated chicken red blood cells (red arrow and 'Ery' within the lumen of this vessel (F, inset). Human specific CD31 immunofluorescence (red) lining the lumen of the printed vessels that is surrounded by αSMA-positive smooth muscle cells (G) and (H). Note that the nucleated blood cells within the lumina of these vessels indicate their connection to the chicken blood circulation. H&E stained section of the transplanted patch in low magnification showing branching vessel pattern (I). Single immunostaining for CD31 (red) and for αSMA (green) of similar a patch area as shown in I (J) and (K) and double immunostaining for human specific CD31 and αSMA in such areas showing CD31-positive (red) endothelial lining, αSMA-positive (green) peri-endothelial cells and nucleated chicken blood cells within the lumen of a printed vessel (L).

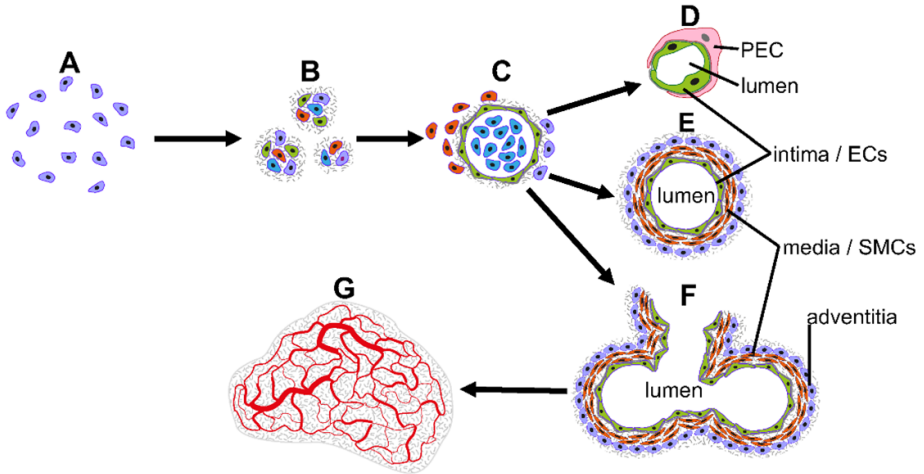

Figure 8. Graphical representation of vascular morphogenesis steps after extrusion-based shape-free printing of hiMPCs that were seeded into the alginate + collagen type I hydrogel into a silicone mold. hiMPCs (blue) seeded into the hydrogel (A), cell sphere formation (like embryonic angioblasts) within the hydrogel (B), lumen formation by relatively flattened cells like ECs (green) with some surrounding cells that probably committed to peri-ECs (red) (C), differentiation and further maturation of vessel-like channels to a capillary phenotype (D) and, branching vessels with multilayered wall structure exhibiting an intima, media and adventitia (F) Within the silicone mold, this vessel-like channels formed a 3D network composed by small and large vessels that displayed a hierarchic organization schematically visualized (G).

as blood vessels *in situ*. To our best expectation, all aforementioned goals were met by using hiMPCs seeded into alginate + collagen type I hydrogel and extruded shape-free into a silicon mold. As documented in the main body of published work regarding biofabrication of blood vessels, mature vascular cells such as EC, e.g. HUVECs [50, 51], human microvascular endothelial cells [52] or SMCs [53] as well as ECs plus fibroblasts [54], HUVECs plus mesenchymal cells plus fibroblasts [55] and HUVECs plus SMCs [8] were used for vascular bioprinting. While these cell types have a vascular phenotype and thus, can be expected to easily form vascular structures, the mature state or character of these cells has to be considered when using them for the biofabrication of new vessels. Due to their mature state ECs, SMCs or fibroblasts cannot run the basic molecular and cellular program as e.g. the so-called angioblasts of mesodermal origin do during *de novo* embryonic vascular development by vasculogenesis [56]. It has also to be considered that the developmental potential of the mesodermal angioblasts is activated and controlled by essential growth factors and cytokines like vascular endothelial growth factor (VEGF), basic fibroblastic factor (bFGF), platelet-derived growth factor (PDGF), and angiopoietin-Tie-2 signaling. Among these factors, the VEGF-VEGF-R2 (FLK1) signaling system is the master regulator of vasculogenesis as studies on gene knock-out models revealed that even mice with a heterozygous deletion of only one allele of the VEGF gene were embryonically lethal due to the severe vascular defects on a very early stage of embryonic development [57, 58]. Moreover, VEGF is not only needed for initial vascular formation but together with PDGF and angiopoietins, it is also needed for further vascular maturation, e.g. by the assembly of peri-ECs such as pericytes and SMCs into the wall of new vessels which leads to vascular stabilization and survival [59]. Based on the aforementioned knowledge, we brought FLK1-positive mesodermal progenitors and bioinks together in a formulation and further added VEGF to our constructs and the culture medium after extrusion to initiate the formation of blood vessel-like structures from hiMPCs. Once primed for differentiation, mesodermal cells give rise to all vascular wall cell types such as ECs, SMCs and MSCs/fibroblasts that in turn can interact with each other and orchestrate the further steps of vascular morphogenesis including a hierarchic vessel system containing both micro- and macrovessels with multilayered vessel wall as demonstrated in this work. We recently used hiMPCs in organoid models where they also provided vascularization [24, 49] underlining the basic vasculogenic potential of hiMPCs. Remarkably, in comparison to the organoids where we observed vessels with only one layer of peri-ECs we achieved in the current study the formation of vessels with multilayered tunica media as demonstrated by histology and electron microscopic analyses. Moreover, in vessels with a diameter of 100–200 μm or above, we also observed an adventitia-like outermost layer similar to the vessels *in situ*. The $CD34^+$ immunophenotype of a part of these adventitial cells underlines also their spatial organization within the vessel wall like blood vessel *in situ* and the $CD34^+$ vascular adventitial cells have been shown to have angiogenic and vasculogenic potential even in adult vessels [21, 60]. The advantage of this approach, as we initially postulated, lies in the fact, that we indeed could mimic the basic steps of embryonic vasculogenesis in a shape-free biofabrication procedure of creating artificial blood vessels as graphically visualized below (figure 8). With this, our approach opens a new avenue for biofabrication of blood vessels by combining technologies of shaped biofabrication + vascular progenitors (iPCs-derived or primary vascular progenitors) + vasculogenic factors. This would enable to improve the simultaneous vascularization of biofabricated tissues and organs on the one side but also improve the cardiovascular as an organ model itself.

5. Conclusion

With the current study, we introduce a new approach in the field of blood vessel biofabrication using (a) human iPSC-derived hiMPCs which were formulated in alginate + collagen type I hydrogel and printed into molds by extrusion, and (b) culture of these constructs in endothelial growth medium by adding VEGF to induce the vascular potential of hiMPCs mimicking the *de novo* blood vessel formation during embryogenesis. We demonstrate that this approach resulted in the formation of small and large vessels with multilayered wall structures displaying intima-, media- and adventitia-like layers. Moreover, the vessels were organized in a hierarchic vascular network by branching in a similar pattern as the vascular system *in situ* and as proof-of-concept the printed vessels were suitable for blood perfusion under *in vivo* conditions when transplanted into the CAM. Adapting this approach to other types of bioinks as well as techniques of bioprinting allowing shaped biofabrication of blood vessels in tissue- and organ-specific pattern under adding essential factors that are indispensable for proper vascular morphogenesis such as VEGF, PDGF, and angiopoietins in future studies would enable a major step forward in achieving the goal of vascularization of biofabricated tissues and organs.

Data availability statement

The data that support the findings of this study are openly available at the following URL/DOI: https://tomviz.org/.

Acknowledgments

This research was funded by the Deutsche Forschungsgemeinschaft (DFG, German Research Foundation)—Project No. 326998133—TRR 225 (subproject B04)

ORCID iDs

Sven Schmidt https://orcid.org/0000-0003-0558-4001
Jürgen Groll https://orcid.org/0000-0003-3167-8466
Süleyman Ergün https://orcid.org/0000-0002-2112-5377

References

[1] Assmann A *et al* 2013 Acceleration of autologous *in vivo* recellularization of decellularized aortic conduits by fibronectin surface coating *Biomaterials* **34** 6015–26
[2] Syedain Z H, Meier L A, Bjork J W, Lee A and Tranquillo R T 2011 Implantable arterial grafts from human fibroblasts and fibrin using a multi-graft pulsed flow-stretch bioreactor with noninvasive strength monitoring *Biomaterials* **32** 714–22
[3] Kumar V A, Caves J M, Haller C A, Dai E, Liu L, Grainger S and Chaikof E L 2013 Acellular vascular grafts generated from collagen and elastin analogs *Acta Biomater.* **9** 8067–74
[4] Li X, Xu J, Nicolescu C T, Marinelli J T and Tien J 2017 Generation, endothelialization, and microsurgical suture anastomosis of strong 1-mm-diameter collagen tubes *Tissue Eng.* A **23** 335–44
[5] Weinberg C B and Bell E 1986 A blood vessel model constructed from collagen and cultured vascular cells *Science* **231** 397–400
[6] Li Y *et al* 2017 Construction of small-diameter vascular graft by shape-memory and self-rolling bacterial cellulose membrane *Adv. Healthcare Mater.* **6** 1601343
[7] Ju Y M, Ahn H, Arenas-Herrera J, Kim C, Abolbashari M, Atala A, Yoo J J and Lee S J 2017 Electrospun vascular scaffold for cellularized small diameter blood vessels: a preclinical large animal study *Acta Biomater.* **59** 58–67
[8] Xu L *et al* 2020 Bioprinting small diameter blood vessel constructs with an endothelial and smooth muscle cell bilayer in a single step *Biofabrication* **12** 045012
[9] Zhang Y, Kumar P, Lv S, Xiong D, Zhao H, Cai Z and Zhao X 2021 Recent advances in 3D bioprinting of vascularized tissues *Mater. Des.* **199** 109398
[10] Fazal F, Raghav S, Callanan A, Koutsos V and Radacsi N 2021 Recent advancements in the bioprinting of vascular grafts *Biofabrication* **13** 032003
[11] Xu Y *et al* 2018 A novel strategy for creating tissue-engineered biomimetic blood vessels using 3D bioprinting technology *Materials* **11** 1581
[12] Itoh M, Nakayama K, Noguchi R, Kamohara K, Furukawa K, Uchihashi K, Toda S, Oyama J I, Node K and Morita S 2015 Scaffold-free tubular tissues created by a bio-3D printer undergo remodeling and endothelialization when implanted in rat aortae *PLoS One* **10** e0136681
[13] Arai K, Murata D, Verissimo A R, Mukae Y, Itoh M, Nakamura A, Morita S and Nakayama K 2018 Fabrication of scaffold-free tubular cardiac constructs using a Bio-3D printer *PLoS One* **13** e0209162
[14] Zhou X, Nowicki M, Sun H, Hann S Y, Cui H, Esworthy T, Lee J D, Plesniak M and Zhang L G 2020 3D bioprinting-tunable small-diameter blood vessels with biomimetic biphasic cell layers *ACS Appl. Mater. Interfaces* **12** 45904–15
[15] Leucht A, Volz A-C, Rogal J, Borchers K and Kluger P J 2020 Advanced gelatin-based vascularization bioinks for extrusion-based bioprinting of vascularized bone equivalents *Sci. Rep.* **10** 5330
[16] Rayatpisheh S, Heath D E, Shakouri A, Rujitanaroj P O, Chew S Y and Chan-Park M B 2014 Combining cell sheet technology and electrospun scaffolding for engineered tubular, aligned, and contractile blood vessels *Biomaterials* **35** 2713–9
[17] Gao G, Park J Y, Kim B S, Jang J and Cho D W 2018 Coaxial cell printing of freestanding, perfusable, and functional *in vitro* vascular models for recapitulation of native vascular endothelium pathophysiology *Adv. Healthcare Mater.* **7** e1801102
[18] Li L, Qin S, Peng J, Chen A, Nie Y, Liu T and Song K 2020 Engineering gelatin-based alginate/carbon nanotubes blend bioink for direct 3D printing of vessel constructs *Int. J. Biol. Macromol.* **145** 262–71
[19] Wörsdörfer P, Mekala S R, Bauer J, Edenhofer F, Kuerten S and Ergün S 2017 The vascular adventitia: an endogenous, omnipresent source of stem cells in the body *Pharmacol. Ther.* **171** 13–29
[20] Patan S 2004 Vasculogenesis and angiogenesis *Angiogenesis in Brain Tumors* (Berlin: Springer) pp 1–30
[21] Zengin E, Chalajour F, Gehling U M, Ito W D, Treede H, Lauke H, Weil J, Reichenspurner H, Kilic N and Ergün S 2006 Vascular wall resident progenitor cells: a source for postnatal vasculogenesis *Development* **133** 1543–51
[22] Ergun S, Hohn H-P, Kilic N, Singer B B and Tilki D 2008 Endothelial and hematopoietic progenitor cells (EPCs and HPCs): hand in hand fate determining partners for cancer cells *Stem Cells Dev.* **4** 169–77
[23] Psaltis P J and Simari R D 2015 Vascular wall progenitor cells in health and disease *Circ. Res.* **116** 1392–412
[24] Wörsdörfer P, Dalda N, Kern A, Krüger S, Wagner N, Kwok C K, Henke E and Ergün S 2019 Generation of complex human organoid models including vascular networks by incorporation of mesodermal progenitor cells *Sci. Rep.* **9** 15663
[25] Sarker M D, Naghieh S, Sharma N K and Chen X 2018 3D biofabrication of vascular networks for tissue regeneration: a report on recent advances *J. Pharm. Anal.* **8** 277–96
[26] Erguen S, Tilki D and Klein D 2011 Vascular wall as a reservoir for different types of stem and progenitor cells *Antioxid. Redox Signal.* **15** 981–95
[27] Zhu W *et al* 2017 Direct 3D bioprinting of prevascularized tissue constructs with complex microarchitecture.pdf *Biomaterials* **124** 106–15
[28] Sommer C A, Stadtfeld M, Murphy G J, Hochedlinger K, Kotton D N and Mostoslavsky G 2009 Induced pluripotent stem cell generation using a single lentiviral stem cell cassette *Stem Cells* **27** 543–9
[29] Kwok C K, Ueda Y, Kadari A, Günther K, Ergün S, Heron A, Schnitzler A C, Rook M and Edenhofer F 2018 Scalable stirred suspension culture for the generation of billions of human induced pluripotent stem cells using single-use bioreactors *J. Tissue Eng. Regen. Med.* **12** e1076–87
[30] Walton J 1979 Lead asparate, an en bloc contrast stain particularly useful for ultrastructural enzymology *J. Histochem. Cytochem.* **27** 1337–42
[31] Cardona A, Saalfeld S, Schindelin J, Arganda-Carreras I, Preibisch S, Longair M, Tomancak P, Hartenstein V and Douglas R J 2012 TrakEM2 software for neural circuit reconstruction *PLoS One* **7** e38011
[32] Schindelin J *et al* 2012 Fiji: an open-source platform for biological-image analysis *Nat. Methods* **9** 676–82
[33] Fonseca C G, Barbacena P and Franco C A 2020 Endothelial cells on the move: dynamics in vascular morphogenesis and disease *Vasc. Biol.* **2** H29–43
[34] Tilki D, Hohn H-P, Ergün B, Rafii S and Ergün S 2009 Emerging biology of vascular wall progenitor cells in health and disease *Trends Mol. Med.* **15** 501–9

[35] Sarker B, Rompf J, Silva R, Lang N, Detsch R, Kaschta J, Fabry B and Boccaccini A R 2015 Alginate-based hydrogels with improved adhesive properties for cell encapsulation *Int. J. Biol. Macromol.* **78** 72–8
[36] Sabin F R 1917 Preliminary note on the differentiation of angioblasts and the method by which they produce blood-vessels, blood-plasma, and red blood-cells as seen in the living chick *Anat. Rec.* **13** 199–204
[37] Ferkowicz M J and Yoder M C 2005 Blood island formation: longstanding observations and modern interpretations *Exp. Hematol.* **33** 1041–7
[38] Risau W and Flamme I 1995 Vasculogenesis *Annu. Rev. Cell Dev. Biol.* **11** 73–91
[39] Matsumoto K *et al* 2001 Liver organogenesis promoted by endothelial cells prior to vascular function *Science* **294** 559–63
[40] Wörsdörfer P and Ergun S 2018 Do vascular mural cells possess endogenous plasticity in vivo? *Stem Cell Rev. Rep.* **14** 144–7
[41] Risau W 1996 What, if anything, is an angiogenic factor *Cancer Metastasis Rev.* **15** 149–51
[42] D'Amore D C D A P A 2001 Cell–cell interactions in vascular development *Dev. Biol.* **52** 107–49
[43] Sweeney M and Foldes G 2018 It takes two: endothelial-perivascular cell cross-talk in vascular development and disease *Front. Cardiovasc. Med.* **5** 154
[44] Davis G E and Senger D R 2005 Endothelial extracellular matrix: biosynthesis, remodeling, and functions during vascular morphogenesis and neovessel stabilization *Circ. Res.* **97** 1093–107
[45] Levenberg S, Zoldan J, Basevitch Y and Langer R 2007 Endothelial potential of human embryonic stem cells *Blood* **110** 806–14
[46] Klein D, Meissner N, Kleff V, Jastrow H, Yamaguchi M, Ergün S and Jendrossek V 2014 Nestin(+) tissue-resident multipotent stem cells contribute to tumor progression by differentiating into pericytes and smooth muscle cells resulting in blood vessel remodeling *Front. Oncol.* **4** 169
[47] Ackermann M, Morse B A, Delventhal V, Carvajal I M and Konerding M A 2012 Anti-VEGFR2 and anti-IGF-1R-Adnectins inhibit Ewing's sarcoma A673-xenograft growth and normalize tumor vascular architecture *Angiogenesis* **15** 685–95
[48] De Spiegelaere W, Casteleyn C, Van Den Broeck W, Plendl J, Bahramsoltani M, Simoens P, Djonov V and Cornillie P 2012 Intussusceptive angiogenesis: a biologically relevant form of angiogenesis *J. Vasc. Res.* **49** 390–404
[49] Wörsdörfer P, Rockel A, Alt Y, Kern A and Ergün S 2020 Generation of vascularized neural organoids by co-culturing with mesodermal progenitor cells *STAR Protoc.* **1** 100041
[50] Norotte C, Marga F S, Niklason L E and Forgacs G 2009 Scaffold-free vascular tissue engineering using bioprinting *Biomaterials* **30** 5910–7
[51] Gao G, Huang Y, Schilling A F, Hubbell K and Cui X 2018 Organ bioprinting: are we there yet? *Adv. Healthcare Mater.* **7** 1701018
[52] Cui X and Boland T 2009 Human microvasculature fabrication using thermal inkjet printing technology *Biomaterials* **30** 6221–7
[53] Schoneberg J, De Lorenzi F, Theek B, Blaeser A, Rommel D, Kuehne A J C, Kießling F and Fischer H 2018 Engineering biofunctional *in vitro* vessel models using a multilayer bioprinting technique *Sci. Rep.* **8** 10430
[54] Bertassoni L E *et al* 2014 Direct-write bioprinting of cell-laden methacrylated gelatin hydrogels *Biofabrication* **6** 024105
[55] Kolesky D B, Homan K A, Skylar-Scott M A and Lewis J A 2016 Three-dimensional bioprinting of thick vascularized tissues *Proc. Natl Acad. Sci. USA* **113** 3179–84
[56] Tomasina C, Bodet T, Mota C, Moroni L and Camarero-Espinosa S 2019 Bioprinting vasculature: materials, cells and emergent techniques *Materials* **12** 2701
[57] Carmeliet P *et al* 1996 Role of tissue factor in embryonic blood vessel development *Nature* **383** 73–5
[58] Ferrara N, Carver-Moore K, Chen H, Dowd M, Lu L, O'Shea K S, Powell-Braxton L, Hillan K J and Moore M W 1996 Heterozygous embryonic lethality induced by targeted inactivation of the VEGF gene *Nature* **380** 439–42
[59] Thurston G, Rudge J S, Ioffe E, Zhou H, Ross L, Croll S D, Glazer N, Holash J, McDonald D M and Yancopoulos G D 2000 Angiopoietin-1 protects the adult vasculature against plasma leakage *Nat. Med.* **6** 460–3
[60] Campagnolo P, Cesselli D, Al Haj Zen A, Beltrami A P, Krankel N, Katare R, Angelini G, Emanueli C and Madeddu P 2010 Human adult vena saphena contains perivascular progenitor cells endowed with clonogenic and proangiogenic potential *Circulation* **121** 1735–45